Darko Veljić[1], Milenko Perović[2], Aleksandar Sedmak[3], Marko Rakin[4], Nikola Bajić[1], Bojan Medjo[4], Horia Dascau[5]

NUMERICAL SIMULATION OF THE PLUNGE STAGE IN FRICTION STIR WELDING

NUMERIČKA SIMULACIJA FAZE URANJANJA KOD ZAVARIVANJA TRENJEM MEŠANJEM

Author's address:
[1] IHIS Science & Technology Park Zemun, Belgrade, Serbia
[2] Chamber of Economy of Montenegro, Podgorica, Montenegro
[3] University of Belgrade, Faculty of Mechanical Engineering
[4] University of Belgrade, Faculty of Technology and Metallurgy
[5] National R&D Institute for Welding and Material Testing, Timisoara, Romania

Keywords
- numerical simulation
- friction stir welding
- plunge stage
- temperature fields

Ključne reči
- numerička simulacija
- zavarivanje trenjem mešanjem
- faza uranjanja
- temperaturna polja

Abstract

This paper investigates the plunge stage using numerical modelling. A three-dimensional finite element model (FEM) of the plunge stage is developed using the commercial code ABAQUS to study the thermo-mechanical processes involved during the plunge stage. A coupled thermo-mechanical 3D FE model uses the arbitrary Lagrangian-Eulerian formulation, the Johnson-Cook material law and Coulomb's Law of friction. The model is developed to study the temperature fields of alloy Al2024-T351 under different process parameters (rotating speed) during the friction stir welding (FSW) process. Numerical results indicate that the maximal temperature of the FSW process can be increased with the increase of rotational speed and that temperature is lower than the melting point of the welding material.

In this analysis, temperature, displacement, and mechanical responses are determined simultaneously. The heat generation in FSW can be divided into three parts: frictional heat generated by the tool shoulder, frictional heat generated by the tool pin, and heat generated by material deformation near the pin region.

Izvod

U ovom radu je istražena faza uranjanja alata primenom numeričkog modeliranja. Trodimenzionalni model konačnih elemenata (FEM) faze uranjanja je razvijen primenom softvera ABAQUS radi proučavanja termomehaničkih procesa koji se odvijaju tokom faze uranjanja. Spregnuti termomehanički 3D FE model se bazira na proizvoljnim formulacijama Lagranža-Ojlera, zakonu materijala Džonson-Kuk i Kulonovom zakonu trenja. Model je razvijen radi proučavanja temperaturskih polja legure Al2024-T351 pod različitim parametrima postupka (brzina rotacije) kod postupka zavarivanja trenjem mešanjem (FSW). Numerički rezultati pokazuju da se maksimalna temperatura postupka FSW može povećati sa povećanjem brzine rotacije, kao i da je temperatura niža od tačke topljenja zavarenog materijala.

U ovoj analizi, temperatura, pomeranje i mehanički odzivi se određuju simultano. Izdvajanje toplote kod FSW se može podeliti na tri dela: toplota trenja koja se razvija kretanjem čela alata, toplota trenja dobijena kretanjem trna alata, kao i toplota usled plastične deformacije materijala u blizini oblasti trna alata.

INTRODUCTION

Friction stir welding has two different stages including a plunge and a linear welding phase, as shown in Fig. 1. In the plunge stage, an FSW tool penetrates the workpieces to be welded. In the linear welding phase, the tool moves along the joint line. This paper investigates the plunge stage using three-dimensional finite element modelling.
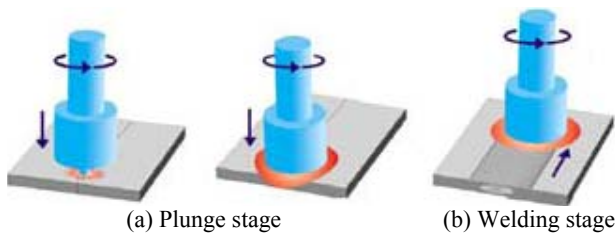
(a) Plunge stage   (b) Welding stage

Figure 1. Friction stir welding process /1/.
Slika 1. Postupak zavarivanja trenjem mešanjem /1/

MATERIAL PROPERTIES

In the present work, the welding plate material is Al 2024-T351. Chemical composition of Al2024-T351: Aluminium (Al) – balance, Cu (4.52), Mg (1.60), Mn (0.65), Fe (0.28), Si (0.12), Zn (0.09), Ti (0.16), Cr (0.01), other total (0.02%), /7/. The thermal and mechanical properties used in this model are given in Table 1. The tool material is steel 155CrVMo121. The backing plate material is steel 42CrMo4.

Table 1. Material properties of Al 2024 T351 /2, 3, 4/.
Tabela 1. Osobine materijala Al 2024 T351 /2, 3, 4/

Material properties	Value
Young's Modulus of Elasticity (GPa)	73.1
Poisson's Ratio	0.33
Initial Yield Stress (MPa)	270
Ultimate Tensile Strength (MPa)	410
Thermal Conductivity (W/mK)	121
Coefficient of Thermal Expansion (°C^{-1})	24.7×10^{-6}
Density (kg/m^3)	2770
Specific Heat Capacity (J/Kg°C)	875
Solidus (°C)	502
Liquidus (°C)	638

MODEL DESCRIPTION

Geometry and finite element mesh

The welding plate dimensions in the numerical model are 50×50 mm and 3 mm in thickness. For three-dimensional numerical model used is the C3D8RT element type, a thermo-mechanically coupled hexahedral element with 8-nodes each having trilinear displacement and temperature degrees of freedom. This element produces uniform strain (first order reduced integration) and contains hourglass control /5/ . The mesh consists of 15276 nodes and 12800 elements. The tool and the backing plate is modelled as a rigid surface having no thermal degrees of freedom. The main tool geometry in the FE model is similar to the experimental tool, Fig. 2. The numerical model of the welding plate, tool, and backing plate is shown in Fig. 3.
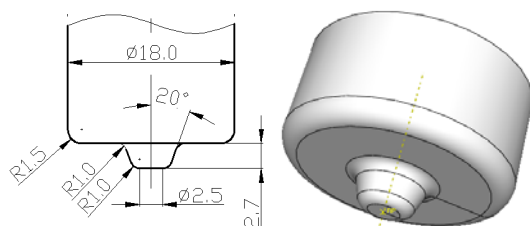

Figure 2. The welding tool used in the experiment and in the numerical analysis.
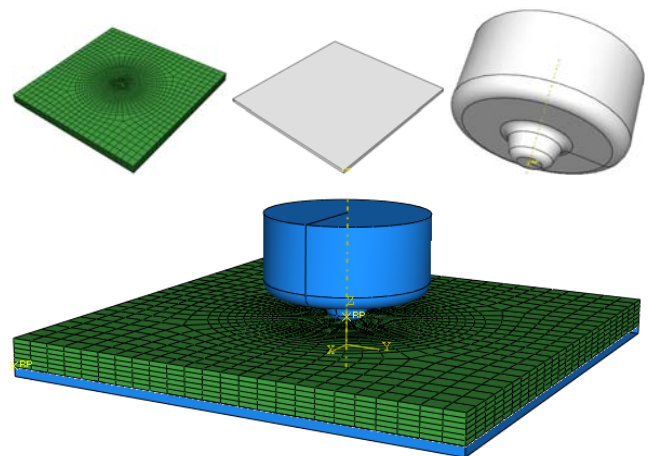Slika 2. Alat za zavarivanje korišćen u eksperimentu i u numeričkoj analizi

Figure 3. Numerical model of welding plate, tool and backing plate.
Slika 3. Numerički model zavarene ploče, alata i podloge

Johnson-Cook elastic–plastic model

In order to avoid the unacceptable mesh distortion caused by the large deformation process, a thermo-mechanical finite element model based on arbitrary Lagrangian-Eulerian formulations and the adaptive meshing are employed in this study. Adaptive meshing in ABAQUS/Explicit /6/ combines features of Lagrangian and Eulerian analyses and is referred to as an ALE analysis. A temperature and strain rate dependent material law is implemented using the elastic-plastic Johnson-Cook material law. The contact forces in the normal direction of the surfaces are modelled by Coulomb's Law of friction. The elastic-plastic Johnson-Cook material law is given by /6/:

$$\sigma_y = \left[A + B(\varepsilon_p)^n \right] \left[1 + C\left(\frac{\dot{\varepsilon}_p}{\dot{\varepsilon}_o} \right) \right] \left[1 - \left(\frac{T - T_{room}}{T_{melt} - T_{room}} \right)^m \right] \quad (1)$$

where: T_{melt} = 502°C –melting point or solidus temperature, T_{room} = 20°C –ambient temperature, T (°C) –effective temperature, A = 265 MPa –yield stress, B = 426 MPa –strain factor, n = 0.34 –strain exponent, m = 1 –temperature exponent, C = 0.015 –strain rate factor. A, B, C, n, T_{melt}, T_{room} and m are material/test constants for the Johnson-Cook strain rate dependent yield stress for Al 2024 T351, /7/.

Thermal model

In general, heat generation comes from two sources: frictional heating at the tool-workpiece interface and from plastic energy dissipation due to shear deformation in the nugget zone. The governing equation for the heat transfer process during the plunge phase of the FSW process can be written as:

$$\rho c \frac{\partial T}{\partial t} = \frac{\partial}{\partial x}\left[k_x \frac{\partial T}{\partial x} \right] + \frac{\partial}{\partial y}\left[k_y \frac{\partial T}{\partial y} \right] + \frac{\partial}{\partial z}\left[k_z \frac{\partial T}{\partial z} \right] + \dot{q}_p \quad (2)$$

where ρ is the density, c –specific heat, k –heat conductivity, T –temperature, t –time, $\dot{q}_p$ is heat generation coming from plastic energy dissipation due to shear deformation, and x, y, and z are spatial coordinates /8/. The rate of heat generation due to plastic energy dissipation, $\dot{q}_p$ is computed from

$$\dot{q}_p = \eta \sigma \dot{\varepsilon}^{pl} \qquad (3)$$

where η is the factor of converting mechanical to thermal energy (0.9) /9/, σ is shear stress, and $\dot{\varepsilon}^{pl}$ is the rate of plastic strain.

Heat generation from frictional heating between tool and workpieces may be written as:

$$\dot{q}_f = \frac{4}{3}\pi^2 \mu P N R^3 \qquad (4)$$

where $\dot{q}_f$ –frictional heat generation, μ –coefficient of friction, P –traction, N –rotational speed, and R –surface radius.

The model is developed to study temperature fields of alloy Al 2024-T351 for different rotating speeds: 320, 400 and 500 min^{-1}, during the plunge stage of the friction stir welding (FSW) process. Figure 4 shows the coordinates of points, T1 (9.5,0,0) and T2(12,0,0), for measuring the temperature dependence of time.
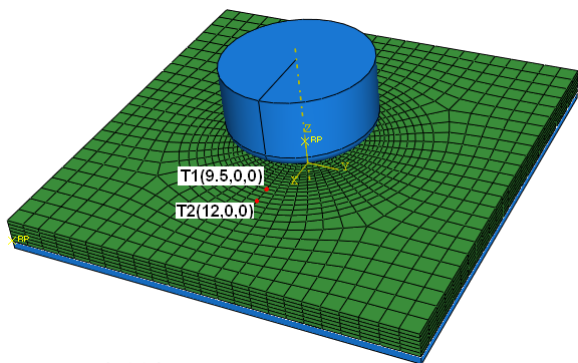

Figure 4. Coordinates of points for measuring temperature dependence of time.
Slika 4. Koordinate tačaka za merenje temperaturske zavisnosti od vremena

RESULTS AND DISCUSSION

Figure 5 shows the temperature fields in the transverse cross section near the tool/matrix interface after 11.6 and 14.5 s, when rotation speed is 320 min^{-1}. The heat transfer through the bottom surface of the workpiece is controlled by the heat transfer coefficient of 1000W/m^{2}K. A constant friction coefficient of 0.3 is assumed between the tool and the workpiece and the penalty contact method is used to model the contact interaction between the two surfaces. Heat convection coefficients on the surface of the workpiece are $h = 10$ W/m^{2}K with ambient temperature of 200°C /9/. This transient temperature field is symmetric.

Figure 6 shows typical temperature distribution over one-half of the workpiece obtained by cutting along transverse directions. It's the temperature field of the plunge stage after 14.5 s when rotation speed is 320 min^{-1}. The plunge depth is 2.9 mm. The tool plunge velocity is set to a uniform value of 0.2 mm/s. This temperature field is symmetric.

Figures 7 and 8 show temperature dependence of time for the plunge stage, when rotation speeds are 320, 400 and 500 min^{-1} in points T1(9.5,0,0) and T2(12,0,0). Numerical results indicate that the temperature in the FSW process can be increased with the increase of rotational speed and that

maximum temperature is lower than the melting point of the welding material (T_{melt} = 502°C, Figs.5 and 6).
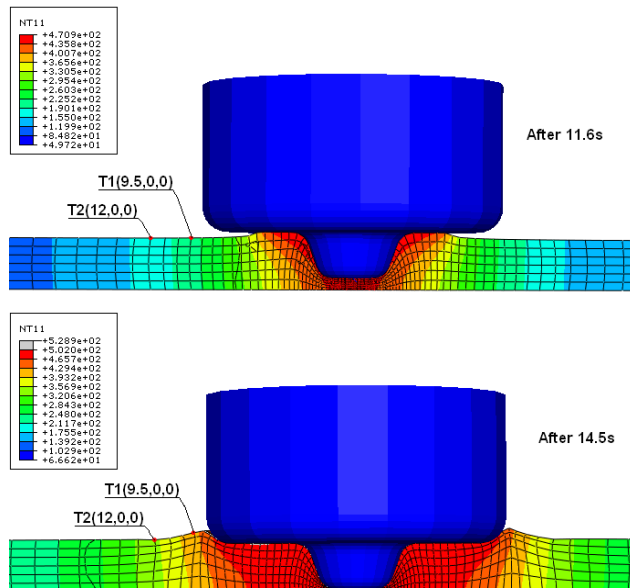

Figure 5. Temperature fields in the transverse cross section near the tool/matrix interface after 11.6 and 14.5 s, when rotation speed is 320 min^{-1}.
Slika 5. Temperaturska polja u poprečnom preseku blizu granice alat/matrica posle 11,6 i '4,5 s, kada je brzina rotacije 320 min^{-1}
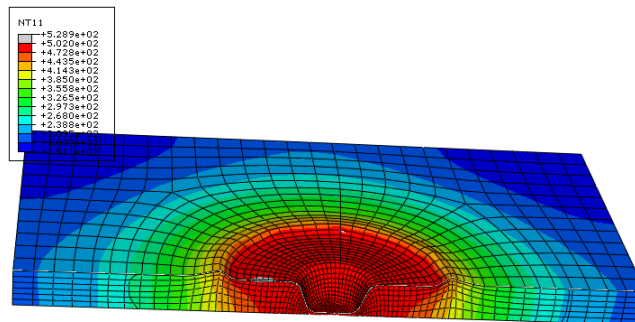

Figure 6. Temperature distribution in aluminium 2024-T351 at the end of an 14.5 s plunge.
Slika 6. Raspodela temperature u aluminijumu 2024-T351 na kraju uronjavanja od 14,5 s
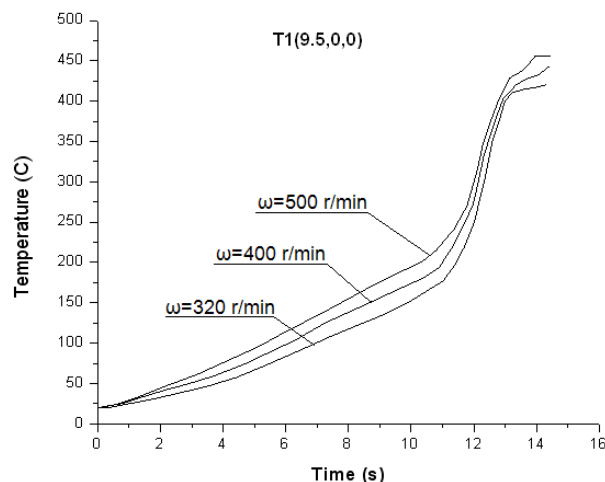

Figure 7. Temperature dependence of time (point T1).
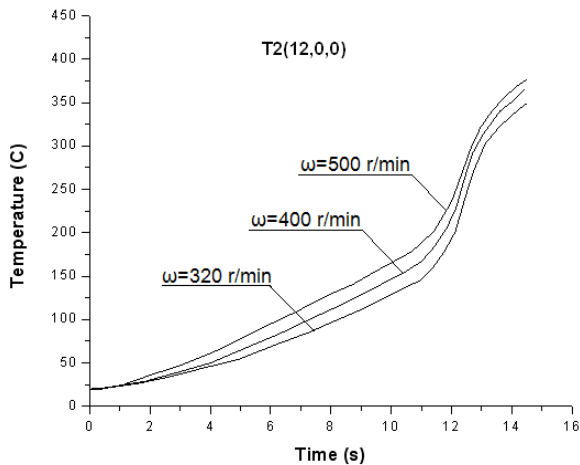Slika 7. Temperaturska zavisnost vremena (tačka T1)

Figure 8. Temperature dependence of time (point T2)
Slika 8. Temperaturska zavisnost vremena (tačka T2)

CONCLUSIONS

When the rotational speed is increased, the region in higher temperature can be increased.

The temperature in the matrix is lower than the melting temperature.

The temperature field is symmetric.

REFERENCES

1. Mahoney, M.W., Mishra, R., Nelson, T., *High Strain Rate Superplasticity in Thick Section 7050 Aluminium Created by Friction Stir Processing*, Proceedings of the Third International Symposium on Fricion Stir Welding, Kobe Exibition Center, Port Island, Kobe, Japan, September 2001 (distributed by TWI on CD).
2. Aluminum 2024-T4; 2024-T351 – ASM Material Data Sheet, http://asm.matweb.com/search/SpecificMaterial.asp?bassnum=MA2024T4
3. Johnson, G.R., Cook, W.H., *A constitutive model and data for metals subjected to large strains, high strain rates and high temperatures*, http://www.ballistics.org/07_01.pdf
4. Certificate conformity, ALCOA International Inc., Approved Certificate No 47831, date 21.10.1990.
5. Zhang, Z., Bie, J., Zhang, H., *Effect of Traverse/Rotational Speed on Material Deformations and Temperature Distributions in Friction Stir Welding*, J Mater. Sci. Technol. 24 (2008) pp.907-913.
6. Abaqus Inc., Analysis - User's Manual v.6.7, 2007.
7. Veljic, D., Perovic, M., Medjo, B., Rakin, M., Sedmak, A., Dascau, H., *Thermo-mechanical modeling of Friction Stir Welding*, The 4th Internat. Conference, Innovative technologies for joining advanced materials, June 10-11, 2010, Proceedings, pp.171-176, on CD.
8. Kwanghyun Park, Development and analisys of ultrasonic assisted friction stir welding process, Doctor of Philosophy (Mechanical Engineering) at The University of Michigan, 2009.
9. Schmidt, H., Hattel, J., A local model for the thermomechanical conditions in friction stir welding, Modelling Simul. Mater. Sci. Eng. 13 (2005) pp.77-93.